Tracking dynamics of magma migration in open-conduit systems

Sebastien Valade[1], Giorgio Lacanna[1], Diego Coppola[2], Marco Laiolo[2], Marco Pistolesi[1], Dario Delle Donne[3], Riccardo Genco[1], Emanuele Marchetti[1], Giacomo Ulivieri[1], Carmine Allocca[1], Corrado Cigolini[2], Takeshi Nishimura[4], Pasquale Poggi[5] and Maurizio Ripepe[1]

[1] *Dipartimento di Scienze della Terra, Università di Firenze (Italy)*

[2] *Dipartimento di Scienze della Terra, Università di Torino (Italy)*

[3] *Dipartimento di Scienze della Terra e del Mare, Università di Palermo (Italy)*

[4] *Department of Geophysics, Tohoku University, Sendai (Japan)*

[5] *Istituto Nazionale di Ottica-CNR, Firenze (Italy)*

Abstract

Open-conduit volcanic systems are typically characterized by unsealed volcanic conduits feeding permanent or quasi-permanent volcanic activity. This persistent activity limits our ability to read changes in the monitored parameters, making the assessment of possible eruptive crises more difficult. We show how an integrated approach to monitoring can solve this problem opening a new way to data interpretation. The increasing rate of explosive transients, tremor amplitude, thermal emissions of ejected tephra, and rise of the very-long-period (VLP) seismic source towards the surface are interpreted as indicating upward migration of the magma column in response to an increased magma input rate. During the 2014 flank eruption of Stromboli this magma input preceded the effusive eruption by several months. When the new lateral effusive vent opened on the Sciara del Fuoco slope**,** the effusion was accompanied by a large ground deflation, a deepening of the VLP seismic source, and the cessation of summit explosive activity. Such observations suggest the drainage of a superficial magma reservoir confined between the crater terrace and the effusive vent. We show how this model successfully reproduces the measured rate of effusion, the

observed rate of ground deflation and the deepening of the seismic VLP source. This study also demonstrates the ability of the geophysical network to detect superficial magma recharge within an open-conduit system, and to track magma drainage during the effusive crisis, with a great impact on hazard assessment.

1. Introduction

Open-conduit volcanoes are characterized by persistent volcanic activity through unsealed volcanic conduits. This implies that such systems do not experience significant internal pressurization, and consequently do not show significant long-term edifice deformation preceding volcanic eruptions (Chaussard et al. 2013). The forecasting of eruptive crises in open systems thus becomes difficult, because monitoring of ground deformation cannot be used to unequivocally identify episodes of new magma addition to magmatic reservoirs.

Stromboli volcano (Italy) is one of the most famous open-conduit basaltic systems. It is well-known for its persistent Strombolian explosive activity which has been ongoing for centuries (Rosi et al. 2000, 2013), characterized by rhythmic mild explosions ejecting lapilli, bombs, ash and a minor lithic component from the active craters. During periods of ordinary activity, the average magma supply rate from depth is 0.1-0.5 m^3/s (Allard et al. 1994; Harris and Stevenson 1997; Ripepe et al. 2005; Burton et al. 2007). This steady-state regime is sometimes interrupted by effusive crises, characterized by the opening of new lateral eruptive vents which feed Mm^3-large, weeks to months-duration lava flows (Barberi et al. 1993, 2009; Marsella et al. 2011). These effusive eruptions have been in the past frequently associated with lateral tsunamogenic landslides occurring immediately before or during the first (hours to days) phases of the effusive eruption (Tinti et al. 2006; Chiocci et al. 2008). Moreover, the persistent activity can also be interrupted by more violent “major” explosions (~2 per year) with the formation of ash- and lapilli-charged plumes up to a few hundred meters high (Barberi et al. 1993; Rosi et al. 2013). More rarely (every 5–10 years), “paroxysmal” explosions forming plumes a few kilometers high can strike the

villages with the fallout of pumice and ballistic blocks (Barberi et al. 1993; Rosi et al. 2013). Our ability to predict all of these events outside the range of the mild persistent Strombolian activity is intimately related to the capability of the monitoring network to track in real-time the migration of magma towards the surface within the shallow portions of the edifice.

The 2014 effusive eruption, which lasted from August 07 until November 22, was the most recent of four important events in the last 30 years (i.e., 1985, 2002-03, 2007, and 2014; De Fino et al. 1988; Calvari et al. 2005, 2010; Barberi et al. 2009). We describe the 2014 eruption using data from a geophysical monitoring network including seismic, infrasonic, tilt, and thermal sensors, deployed and operated by the University of Firenze (UNIFI) since 2003 (Ripepe et al. 2004). Additionally, we integrate lava discharge rate data retrieved from satellite thermal images (Coppola et al. 2013, 2015). In the present study, we demonstrate the ability of the network to detect the magma recharge and discharge processes in the shallow conduit system, as well as its ability to track the migration of magma within the conduit system. We provide a quantitative model to explain the data collected during the effusive eruption as the discharge of a shallow reservoir, and we suggest an interpretative model of Stromboli's magma recharge/drainage cycles, eventually discussing the model's implications for hazards assessment.

2. Monitoring geophysical network

The monitoring network operated by the Laboratorio di Geofisica Sperimentale (LGS) of the UNIFI was deployed in January 2003, and it has been in continuous expansion ever since (Ripepe et al. 2004, 2005, 2007, 2009; Figure 1a). It currently consists of 4 seismo-acoustic stations (ROC, PZZ, STR, SCI), 1 five-element infrasonic array (EAR), 2 thermal infrared cameras (ROC, GST), 4 tiltmeters (bore-hole: OHO, LSC, LFS, surface: CPL), and 1 gauge for tsunami monitoring (PDC). All data are radio transmitted to the monitoring center of the Department of the Civil Protection (COA) on the island, where data are collected, processed and published in real-time on the web. In addition, thermal satellite remote sensing using the Moderate Resolution Imaging

Spectroradiometer (MODIS) sensor is achieved through MIROVA (Middle InfraRed Observation of Volcanic Activity), in collaboration with the University of Torino (Coppola et al. 2015).

3. Geophysical evidence of magma recharge/discharge process

The 2014 flank eruption provided high-quality geophysical data on processes occurring within the shallow feeding system of Stromboli. The eruptive crisis is hereafter described in 3 main phases: 1) the months-long pre-effusive recharging phase, characterized by the progressive increase in explosive activity at the summit craters; 2) the effusive onset, marked by a small lava flow originated from the partial collapse of the NE1 crater on August 6, followed by the opening of a new lateral effusive vent on August 7, and 3) the weeks-long effusive discharging phase, characterized by a gradual decrease in the lava effusion rate.

3.1. Pre-effusive phase: magma recharge

Nearly 4 months prior to the eruption onset, most of the geophysical parameters started to outline an escalation in the explosive activity. The tremor amplitude gradually increased (Figure 2a), along with the rate of very-long-period (VLP, 10-20 sec period) seismic activity (black curve in Figure 2b). This trend was associated with the decrease of the VLP polarization dip angle (blue curve in Figure 2b), calculated as the angle between the main axis of the polarization vector of the seismic VLP and the horizontal plane (Marchetti and Ripepe 2005; Ripepe et al. 2015) at station STR. Thus, the decrease of the polarization dip angle indicates a migration of the position of the VLP seismic source towards the surface. The acoustic pressure of the explosions also increased (Figure 2d), together with thermal measurements from both ground- and satellite-based sensors (Figure 2e, f), which indicate an increase in frequency and intensity (tephra volume and exit velocities) of the explosions, resulting in a larger amount of hot material emitted from the summit craters. Tephra volumes and exit velocities in particular, are estimated by real-time processing of thermal camera data, as described in Delle Donne and Ripepe (2012). It is worth noting that this increase in the

105 monitored parameters and explosive activity followed a local earthquake of moderate size (M_L =
106 2.5) at 6.2 km below the edifice on May 26, 2014 (INGV Centro Nazionale Terremoti).
107 During this period of increased activity nine short-lived lava overflows were recorded (Figure 2,
108 orange stripes) from the active vents, which remain mostly confined within the crater terrace or in
109 the upper part of the Sciara del Fuoco. Most overflows in 2014 were characterized by the same
110 distinctive features: increasing spatter activity from the NE1 crater, accompanied by a rapid
111 increase in both tremor amplitude (Figure 3a) and infrasonic pressure (Figure 3b), with no
112 significant ground inflation. As the spattering activity reached the maximum rate of 1-2
113 explosions/second, the infrasonic activity shifted from the central crater towards the NE1 crater
114 (Figure 3d). Simultaneously, when lava overflowed from the crater onto the Sciara del Fuoco, all
115 tiltmeters detected a clear ground deflation, of amplitude typically <0.2 μm at OHO station (Figure
116 3c, Supplementary Material) indicating the decompression of the magmatic system. Tremor
117 amplitude and infrasonic pressure continued to increase during the decompression until the
118 maximum deflation was reached (Figure 3). This possibly suggests that the overflow itself
119 enhances explosive/spattering activity by decompressing the magmatic system after the removal
120 of the upper part of the magma column.
121 Three days prior to the eruption onset, on August 3, the explosive activity increased significantly,
122 as shown by large infrasonic pressure, high VLP rate, and the amount of ejected tephra volumes
123 (Figure 2b, 2d and 2e).
124 The simultaneous increase of all the monitored geophysical parameters suggests that an increase
125 of the magma/gas input rate already started ~4 months prior to the effusive eruption onset, forcing
126 the magma column towards the surface, as shown by the gradual upward migration of the VLP
127 seismic source. This lead to a progressive increase of the explosive activity and to the numerous
128 overflows recorded during this period.
129
130 **3.2. Effusive onset: vent opening**

The onset of the effusive eruption is marked by the opening of a lateral effusive vent along the Sciara del Fuoco on August 07, 2014 at 05:00 GMT (solid red line in Figure 4). However, the vent opening was preceded by a complex phase which lasted nearly 15 hours. This phase initiated with the collapse of a portion of the NE1 crater rim (dashed red line in Figure 4), generating a large rockfall on the Sciara del Fuoco which was detected by all the seismic stations. This collapse initiated a small lava flow which reached the sea in a few hours. During this short-lived lava flow from the NE1 crater, the explosive activity decreased significantly, as indicated by the drop of the tremor amplitude, the rate and the pressure of infrasonic transients (Figure 4a, d). This drop is also accompanied by a short deflation of 0.52 µrad at the OHO tiltmeter (black curve in Figure 4c). Moreover, during the 15 hours following the collapse of the NE1 crater, the CPL tiltmeter recorded a progressive ground inflation of ~13 µrad (blue curve in Figure 4c), which culminated on 07 August 2014 at ~05:00 GMT with the opening of a new effusive vent on the lower parts of the NE2 crater flank at ~670 m a.s.l. (Figure 1). The CPL tiltmeter, located 200 m from the new effusive vent, is the only one to have recorded this phenomenon with such intensity, implying a very localized and shallow source, which is consistent with the intrusion of a very shallow lateral dyke from the main conduit towards the northern flank of the edifice.

The opening of the new effusive vent was associated with a peak in the seismic tremor (Figure 4a) which was not accompanied by an increase in infrasound activity, indicating that the seismic source was not coupled with the atmosphere and most probably related to the migration of the magma within the dyke. The migration of the magma from the summit craters towards the new effusive vent probably contributed to reduce the magma static pressure working on the crater rims and possibly caused their instability which culminated with the rockfall of August 6.

3.3. Effusive phase: magma drainage

Following the vent opening, volcanic activity and geophysical parameters changed drastically, reflecting the shift from the explosive to the effusive regime. Effusive rates estimated from the

analysis of MODIS thermal images shows a peak of >20 m^3/s, resulting in ~$1.6x10^6$ m^3 of lava emitted in the first two days (Figure 5e). During this phase, all tiltmeters recorded a large and rapid ground deflation (~7 μrad in 48 hours at OHO station and ~26 μrad at CPL station, respectively black and blue curve in Figure 5c). As the explosive activity at the summit craters ceased, the tremor amplitude dropped, and both infrasonic and thermal transients were not recorded anymore. In addition, while the rate and amplitude of VLP seismic activity remained high (Figure 5b, black curve), the polarization dip angle of the VLP increased by approximately 3° with respect to pre-effusive condition, indicating the deepening of the VLP source depth (Figure 5b, blue curve).

From August 9 (three days after the eruption onset) onwards, activity and geophysical parameters remained stable: low tremor amplitude, no infrasonic activity, no thermal signals linked to the explosive activity, and a sustained VLP rate yet with a deep source location. The effusion rate estimated from MODIS images showed an exponential decrease during the first month, reaching steady values of 0.2-0.4 m^3/s from mid-September. The camera pointing at the effusive vent showed that it remained stable at ~670 m a.s.l. until the end of the eruption, which finally ceased on 22 November 2014.

The exponential decreasing trends of tilt, effusion rate, and VLP dip during the first 48 hours suggest the rapid drainage of a shallow reservoir, which is consistent with the progressive internal collapse of the craters reported from field observations and thermal infrared camera surveys (Figure 6).

4. Model of magma discharge

We explain all the recorded geophysical parameters by using a dynamical model based on the migration of the magma column within the shallow conduits. We assume that during the months preceding the effusive onset, magma was accumulated in a shallow reservoir, which was then suddenly drained out from the newly opened effusive vent. The reservoir drainage process can be modeled as the discharge of a cylindrical conduit confined between the new effusive vent and the

crater terrace (Ripepe et al. 2015). If the magma is flowing out the vent through a dyke as a Poiseuille flow, neglecting the effect of the atmospheric pressure, the velocity *u(t)* at which lava is flowing out the vent can be expressed as:

$$u(t) = \frac{a^2}{4\eta L} P_h(t) \quad (1)$$

where *a* is the effusive vent radius, η is the magma viscosity, and *L* is the dyke length. In this case, the peak pressure at the vent P_h is controlled by the change in the magmastatic pressure gradient in the reservoir, such as $P_h(t) = \rho g h(t)(1-\Phi)$, where *h(t)* is the magma level height above the vent, ρ is the DRE magma density, Φ is the magma vesicularity, and *g* is the acceleration due to gravity. The effusion rate of the lava drained out the reservoir $Q_R(t)$ can be expressed as:

$$Q_R(t) = \pi a^2 u(t) = (1-\Phi)\frac{\pi a^4}{8\eta L} \rho g h(t) \quad (2)$$

which explains that when the lava is drained out the vent, the magma level *h(t)* in the reservoir will progressively drop, from the maximum reservoir height h_0 to the elevation of the effusive vent (670 m a.s.l.). However, the discharge of the reservoir is likely buffered by the magma supply rate from depth Q_D, which is continuously feeding the shallow reservoir also during the eruption. The total lava output rate Q_T at the vent is therefore controlled by the balance between the rapid drainage of the shallow reservoir Q_R, and the constant deep magma input rate Q_D, such as $Q_T(t) = Q_R(t)+Q_D(t)$.

This model was first proposed to explain the 2007 lava flow at Stromboli (Ripepe et al. 2015) and has recently been applied also to the 2014 eruption (Zakšek et al. 2015). In agreement with previous papers, we thus used magma physical parameters typical for Stromboli, such as viscosity $\eta = 10^4$ Pa (Métrich et al. 2001), and dense rock equivalent (DRE) density $\rho = 2{,}950$ kg/m^3 (Pioli et al. 2014), whereas parameters like the radius of the effusive vent *a* = 2 m was measured from the thermal images. Considering magma vesicularity Φ can vary between 0 and 0.45 (Landi et al.

206 2009), we found that the best fit between the modeled and the measured data is reached for a dyke
207 length L = 30 m and the reservoir height h_0 = 47±10 m.
208 If no magma is considered to be supplied from depth (Q_D = 0), the magma static pressure will
209 rapidly drain all the magma out of the shallow reservoir in a few days (Ripepe et al. 2015) and the
210 model will fail to explain the long lasting effusion rate and the volume of the extruded magma
211 (Figure 7b, dashed blue line). Therefore, a magma supply rate from depth has to be considered to
212 recharge the shallow reservoir also during the effusive magma discharge phase. While for the 2007
213 eruption a constant Q_D = 0.7 m^3/s has been successfully used to fit both effusion rate and
214 discharged magma volume (Ripepe et al. 2015), for the 2014 eruption the constant Q_D = 0.4 m^3/s
215 well explains the effusion rate (Zakšek et al. 2015) but fails to reproduce the 107 days long volume
216 of discharged magma (Figure 7, solid blue line).
217 We found that the linear decrease of Q_D from 0.6-0.85 m^3/s at the onset of the eruption, to 0.3 m^3/s
218 at the end of the eruption (typical during the ordinary explosive activity at Stromboli, e.g. Ripepe
219 et al. 2005; Burton et al. 2007) best fits both the effusion rate and discharged volume trends
220 measured by MODIS (respectively Figure 7a and 7b, red curves).
221 The rapid drainage process modeled by the gravity-induced discharge of the shallow reservoir is
222 also in agreement with both the rapid deepening of the seismic VLP source and the rapid ground
223 deflation observed during the first days (Figure 8a and 8b). In particular, if we assume that the
224 effusive eruption results from the emptying of a shallow reservoir located above the effusive vent,
225 this model provides a simple explanation to the deepening rate of the VLP source, which is
226 associated with the progressive drop of the magma level in the shallow reservoir and with the
227 subsequent decrease of the residual magma volume (Figure 8a). This also suggests that VLP is
228 likely generated at the top of the magma column. Moreover, the emptying of the shallow reservoir
229 induces a decompression of the system, which explains why the modeled effusion rate fits the
230 observed ground deformation rate (Figure 8b). This suggests a shallow position of the deformation
231 source (likely above 500 m a.s.l., e.g. Marchetti et al. 2009; Ripepe et al. 2015) rather than deep

source (>1 km below sea level, e.g. Bonaccorso 1998). Finally, the progressive decrease of the input rate during the months following the effusive onset induces a decrease of the magma pressure at the vent, which, as already observed for the 2002-2003 eruption (Ripepe et al. 2005), ultimately results in the vent closure only when the magma input rate decreases back to the stationary 0.3 m^3/s value of magma input rate which characterizes the ordinary explosive activity.

5. Discussion

Measurements of the SO_2 gas flux indicate that the shallow system sustaining the Strombolian activity is continuously fed by a deep magma supply rate of 0.1–0.5 m^3/s (e.g. Burton et al. 2009). However, gas/mass fraction shows that only ~10% of the magma is ejected during the explosive activity, suggesting that almost 90% of the magma supplied remains in the feeding conduits (Allard et al. 1994; Harris and Stevenson 1997; Allard et al. 2008). This degassed magma is inducing a density convection conduit dynamics (Stevenson and Blake 1998; Landi et al. 2004) keeping the feeding system at an equilibrium. When the magma input rate increases, this equilibrium is lost. During such periods of higher magma recharge, the excess of magma confined within the edifice is exclusively dissipated throughout the explosive activity at the summit craters, which is however not able to evacuate the larger volumes of new magma supplied. The increased magma static pressure associated with the increased level of magma in the conduit is likely to induce magma migration into dykes (or sills) and eventually lead to the opening of effusive vents on the flank of the edifice. The geophysical data collected during the recent 2014 eruption is consistent with such scenario, i.e., a process of magma recharge and drainage of a shallow reservoir.

The higher supply of magma to the shallow reservoir is recorded months before the effusive onset, and is responsible for the progressive transition towards a higher explosive regime (Figure 9a) with respect to the usual Strombolian activity. Besides lava overflows, the main geophysical evidence of the response of the shallow conduit system to this higher magma supply rate are: (1)

the increasing number of eruptive vents, (2) the increased rate of explosive activity recorded by thermal sensors; (3) the increase of tremor amplitude and infrasonic pressure, and (4) the migration of the seismic VLP source towards the surface. The effusive onset, typically lasting <24 hours, is characterized by the lateral propagation of shallow dykes, evidenced by both (1) localized ground inflation, and (2) increased landslide activity. When the dyke reaches the surface, it opens a new effusive vent from which lava is drained out of the shallow conduit system. The shift from explosive to effusive regime is then recorded as: (1) the absence of thermal and infrasound transients; (2) the decrease of tremor amplitude; (3) the large ground deflation, and (4) the deepening of the source of VLP seismicity. The direct consequence of the transition to the effusive regime is the progressive collapse of the crater terrace revealing the gravitational instability induced by the large amount of drained magma from the shallow portion of the conduit system.

These observations were modeled as the consequence of the gravity-driven discharge process of a shallow reservoir (Ripepe et al. 2015). The good fit between the modeled effusion rate and the one measured from satellite (Figure 7), suggests that the largest part of the lava emplaced during the first days was already stored in a shallow reservoir confined above the effusive vent. This model also explains the rapid deepening of the seismic VLP source (Figure 8a) and the ground deflation measured by the tiltmeters (Figure 8b).

This gravity-driven process proposed to explain small lateral eruptions at Stromboli (Ripepe et al., 2015; Zakšek et al., 2015) has been used to describe and model geophysical observations of other mafic volcanic larger scale eruptions. At Kīlauea volcano, lateral eruption rate from Kīlauea's East Rift Zone has shown to scale with changes in the Halemaʻumaʻu lava lake level and summit deformation (Patrick et al. 2015). At Nyamulagira volcano, the collapse of the summit pit-crater was associated with waning lateral effusion rates (Coppola et al. 2016a), and more recently, the large effusive eruption at Bárdarbunga volcano has shown lateral effusion rate to correlate with caldera subsidence (Coppola et al. 2016b; Gudmundsson et al. 2016). These similarities suggest that lateral magma effusion rates are controlled by variations in the magma column level, and that

tracking this level using geophysical parameters such as the VLP seismicity, the lava lake level, or the caldera subsidence becomes fundamental for monitoring effusive eruption on a volcano's flank.

6. Hazards implications

During the pre-eruptive (magma recharging) phase, in response to the higher magma supply, the edifice slowly deforms (Figure 9). Although clear inflation trends are difficult to identify (probably because inflation is too slow and thus easily masked by seasonal ground deformation and earth tides), the mean rate of rockfall events usually increases in the late stage and immediately before opening of the effusive vent, reflecting a general flank instability (Marchetti et al. 2009; Di Traglia et al. 2014). As previously observed during the onset of the 2002-2003 eruptive crisis, the inflation may lead to large landslides triggering tsunami waves that may affect the coast of Sicily and Calabria (Tinti et al. 2006; Chiocci et al. 2008).

The supply of magma at increased rate is also responsible for increased explosive activity, and the risk of new vent opening becomes very high. Interestingly, the effusive vents opened during the effusive crisis of 2003, 2007 and 2014 were all located northeast of the SW-NE crater alignment. This crater alignment is thought to result from the orientation of the feeding dike, which follows well-known regional tectonic alignments (Rosi 1980; Hornig-Kjarsgaard et al. 1993; Keller et al. 1993; Tibaldi 2001). The fact that new effusive vents systematically open to the north-east is likely the result of a relatively shallow structural factor: the southwest border of the crater terrace is confined by an old collapse scar acting as a rigid boundary, whereas the northeast border is composed of loose pyroclastic material ejected from the NE crater sector (Tibaldi 2001).

Once the eruptive vent opens, the entire system depressurizes following the effusion rate, and there is overall deflation of the edifice. In this phase, the main hazard is thus no longer the flank instability and potential generation of tsunamis, but processes taking place during the recovery of equilibrium in the magmatic system, in response to the drainage of the uppermost portion of the

edifice. During the effusive crises of 2003 and 2007, violent paroxysmal eruptions occurred during this recovery, ejecting blocks which fell at an elevation of 450 m a.s.l., 1 km from the craters on the northeastern slope, and as far as the village of Ginostra (~2 km from the crater area) on the western slope (Rosi et al. 2006; Pistolesi et al. 2011). These events are commonly explained as resulting from the rapid ascent of parcels of a deep-seated (7-9 km), gas-rich low-porphyricity (LP) magma which eventually interacts with a shallow (2-3 km), high-porphyricity (HP) reservoir (Bertagnini et al. 2003; Métrich et al. 2009). Calvari et al. (2011) suggested that during effusive eruptions the removal of a large volume of magma (~$6.5x10^6$ m^3 of 16-32 vol.% vesicular lava) from the shallow reservoir can be responsible for paroxysmal eruptions. Following the 2014 eruption, ~$5.5x10^6$ m^3 of lava were emplaced in 107 days but no paroxysmal eruption occurred. Although the critical value suggested by Calvari et al. (2011) was not reached, the longer duration over which the total volume was emplaced in 2014 suggests that the controlling factor of such paroxysms may be the rate at which magma is drained out rather than the total volume of magma erupted. Based on this observation we infer that decompression induced by rapid removal of magma from the conduit system (that is large volumes in short time) could be responsible for triggering violent explosive paroxysms at Stromboli.

Figure captions

Figure 1. Shaded relief map of Stromboli volcano. (a) Location of the geophysical sensors and extent of the 2014 lava flow in red. (b) Location of the main craters (SW=South-West crater, C=Central crater, NE1=North-East 1 crater, NE2=North-East 2 crater), and of the new eruptive vent opened on August 7 2014 which fed the lava flow. Digital elevation model computed from images taken in 2014, courtesy of Italian Civil Protection.

Figure 2. Evolution of the geophysical parameters 4 months prior to onset of effusion (01 April – 07 August 2014), and 1 month afterwards (07 August – 01 September 2014). The parameters highlight increasing explosive activity, evidenced by: increasing seismic tremor (a), increasing rate and dip of VLP seismicity (black and blue curve respectively) (b), increasing infrasonic pressures (d), increasing tephra emissions from ground-based (e) and satellite-based (f) thermal sensor. The ground deformation (c) from borehole tilt meter does not show large-scale ground inflation prior to the onset of effusion. The red vertical bar indicates the timing of the eruption onset, corresponding to opening of the new effusive vent on August 07, 2014. The orange vertical bars indicate the timing of the overflow events, and the blue vertical bar the timing of local earthquake recorded on May 26, 2014.

Figure 3. Evolution of geophysical parameters during two overflow events (highlighted in gray) recorded on July 07 2014: (a) seismic tremor, (b) infrasonic pressures, (c) ground deformation, (d) infrasonic sound azimuth, (e) projection of sound azimuth onto digital elevation model, (f) snapshot of the thermal infrared camera ROC as lava overflows from the NE1 crater onto the upper portion of the Sciara del Fuoco. The time of the snapshot is indicated by a green bar in the timeseries (a-d), and a green arrow in plot (e) indicates the corresponding infrasound azimuth.

Figure 4. Evolution of the geophysical parameters a few days prior to and after the onset of effusion. The dashed vertical red bar indicates the time when a portion of the NE1 crater collapsed, and the onset of a small lava flow. Nearly 15 hours afterwards, a new effusive vent opened (2014-08-07 05:00 GMT) as indicated by the solid red line. During this time interval ground inflation was recorded at CPL tiltmeter, as well as a drop in the infrasonic pressures and volcanic tremor.

Figure 5. Evolution of the geophysical parameters following the onset of effusion. The parameters show drastic changes following the new vent's opening: (a) drop of seismic tremor amplitude, (b) deepening of VLP seismicity yet very high VLP rate, (c) exponential ground deflation, (d) decrease and cessation of infrasonic activity, (e) exponential decay of the lava effusion rate. The solid red bar indicates the time when the new vent opened (2014-08-07 05:00 GMT), preceded nearly 15 hours before (dashed vertical red bar) by the collapse of a portion of the NE1 crater and the onset of a small lava flow.

Figure 6. Thermal infrared camera surveys during the months following the onset of effusion (T_0), showing a progressive internal collapse of the crater walls. (Images recorded with a Flir SC660).

Figure 7. Modeling of the effusion rate and volumes of lava based on the gravity-driven discharge of a shallow reservoir confined between the eruptive vent (670 m a.s.l.) and the crater terrace (770 m a.s.l.). (a) Measured and modelled effusion rate during the first 10 days following the lava onset, and (b) measured and modelled cumulative lava volume emitted during the entire effusive period. The black curves represent the measured data (MODIS), and red/blue curves the modelled data. Red curves consider a linearly decreasing Q_D value throughout the effusive period (with magma vesicularities respectively of Φ=0, Φ=0.3 and Φ=0.4), while blue curves consider a constant Q_D value (Q_D=0 m^3/s dashed blue, Q_D=0.4 m^3/s solid blue).

Figure 8. (a) Comparison between the measured deepening of the VLP seismicity (black), and the modeled decay of magma volume in the reservoir following the vent opening (red). (b) Comparison between the ground deflation measured at OHO tiltmeter (black), and the modeled effusion rate following the vent opening (red). The red dashed curves take account for magma vesicularity Φ=0 and Φ=0.4 respectively.

Figure 9. Interpretive sketch of the magma recharge and discharge dynamics suggested from geophysical observations, and implications for associated hazards.

Acknowledgments

We wish to thank Salvatore Zaia and Vivian Anceschi for their continuous support at the Centro Operativo Avanzato of Stromboli (COA). This work was supported by the Italian Civil Protection in the framework of the DEVNET project. The paper has been improved by constructive comments by the Associate Editor Matthew Patrick, the reviewer Matt Haney, and an anonymous reviewer, all of whom we wish to thank.

References

Allard P, Aiuppa A, Burton M, Caltabiano T, Federico C, Salerno G, La Spina A (2008) Crater gas emissions and the magma feeding systemof Stromboli volcano. In: Calvari S, Inguaggiato S, Ripepe M., Rosi M. (ed) The Stromboli Volcano: An Integrated Study of the 2002–2003 Eruption. AGU, Washington DC, Geophysical Monograph Series, 182:65–80. doi:10.1029/182GM07

Allard P, Carbonnelle J, Métrich N, Loyer H, Zettwoog P (1994) Sulphur output and magma degassing budget of Stromboli volcano. Nature 368:326–330. doi:10.1038/368326a0

Barberi F, Civetta L, Rosi M, Scandone R (2009) Chronology of the 2007 eruption of Stromboli and the activity of the Scientific Synthesis Group. J Volcanol Geotherm Res 182(3-4):123-130. doi:10.1016/j.jvolgeores.2008.09.019

Barberi F, Rosi M, Sodi A (1993) Volcanic hazard assessment at Stromboli based on review of historical data. Acta Vulcanol 3:173-187

Bertagnini A, Métrich N, Landi P, Rosi M (2003) Stromboli volcano (Aeolian Archipelago, Italy): An open window on the deep-feeding system of a steady state basaltic volcano. J Geophys Res 108-7:1-15. doi:10.1029/2002JB002146

Bonaccorso S (1998) Evidence of a dyke-sheet intrusion at Stromboli volcano inferred through continuous tilt. Geophys Res Lett 25(22):4225–4228. doi:10.1029/1998GL900115

Burton M, Allard P, Mure F, La Spina A (2007) Magmatic gas composition reveals the source depth of slug-driven strombolian explosive activity. Science 317(5835):227-230. doi: 10.1126/science.1141900

Burton M, Caltabiano I, Mure E, Salerno G, Randazzo D (2009) SO2 flux from Stromboli during the 2007 eruption: Results from the FLAME network and traverse measurements. J Volcanol Geotherm Res 182(3-4):214-220. doi:10.1016/j.jvolgeores.2008.11.025

Calvari S, Lodato L, Steffke A, Cristaldi A, Harris AJL, L. S, E. B (2010) The 2007 Stromboli flank eruption: event chronology and effusion rates using thermal infrared data. J Geophys Res 115(B04201). doi: 10.1029/2009JB006478

Calvari S, Spampinato L, Bonaccorso A, Oppenheimer C, Rivalta E, Boschi E (2011) Lava effusion - A slow fuse for paroxysms at Stromboli volcano? Earth Planet Sci Lett 301(1-2):317-323. doi:10.1016/j.epsl.2010.11.015

Calvari S, Spampinato L, Lodato L, Harris AJL, Patrick MR, Dehn J, Burton MR, Andronico D (2005) Chronology and complex volcanic processes during the 2002–2003 flank eruption at Stromboli Volcano (Italy) reconstructed from direct observations and surveys with a hand-held thermal camera. J Geophys Res 110:B02201. doi:10.1029/2004JB003129

Chaussard E, Amelung F, Aoki Y (2013) Characterization of open and closed volcanic systems in Indonesia and Mexico using InSAR time series. J Geophys Res Solid Earth 118:1-13. doi:10.1002/jgrb.50288

Chiocci FL, Romagnoli C, Tommasi P, Bosman A (2008) The Stromboli 2002 tsunamigenic submarine slide: Characteristics and possible failure mechanisms. J Geophys Res Solid Earth 113(10):B10102. doi:10.1029/2007JB005172

Coppola D, Campion R, Laiolo M, Cuoco E, Balagizi C, Ripepe M, Cigolini C, Tedesco D (2016) Birth of a lava lake: Nyamulagira volcano 2011–2015. Bull Volcanol 78(3):1-13. doi:10.1007/s00445-016-1014-7

Coppola D, Laiolo M, Cigolini C, Barsotti S, Jónasdóttir E, Ripepe M (2016) Effusion rates, volumes and emplacement style using MODIS MIR data: the 2014-15 Holuhraun eruption (Bárðarbunga, Iceland) tracked by MIROVA. EGU General Assembly 2016 18:EGU2016-16308

Coppola D, Laiolo M, Cigolini C, Delle Donne D, Ripepe M (2015) Enhanced volcanic hot-spot detection using MODIS IR data: results from the MIROVA system. In: Harris AJL, De Groeve T, Garel F, Carn SA (ed), Detecting, Modelling and Responding to Effusive Eruptions. Geological Society, London, Special Publications 426. doi:10.1144/SP426.5

Coppola D, Laiolo M, Piscopo D, Cigolini C (2013) Rheological control on the radiant density of active lava flows and domes. J Volcanol Geotherm Res 249:39–48. doi:10.1016/j.jvolgeores.2012.09.005

De Fino M, La Volpe L, Falsaperla S, Frazzetta G, Neri G, Francalanci L, Rosi M and Sbrana A (1988) The Stromboli eruption of December 6, 1985 - April 15, 1986: volcanological, petrological and seismological data. Rendiconti della Società Italiana di Mineralogia e Petrologia 43:1021-1038

Delle Donne D, Ripepe M (2012) High-frame rate thermal imagery of strombolian explosions: Implications for explosive and infrasonic source dynamics. J Geophys Res Solid Earth 117(9):B09206. doi:10.1029/2011JB008987

Di Traglia F, Nolesini T, Intrieri E, Mugnai F, Leva D, Rosi M, Casagli N (2014) Review of ten years of volcano deformations recorded by the ground-based InSAR monitoring system at Stromboli volcano:

454 a tool to mitigate volcano flank dynamics and intense volcanic activity. Earth-Sci Rev 139:317-335.
455 doi:10.1007/s00445-013-0786-2
456 Gudmundsson MT et al. (2016) Gradual caldera collapse at Bárdarbunga volcano, Iceland, regulated by
457 lateral magma outflow. Science 353 (6296). doi:10.1126/science.aaf8988
458 Harris AJL, Stevenson DS (1997) Magma budgets and steady-state activity of Vulcano and Stromboli
459 volcanoes. Geophys Res Lett 24:1043–1046. doi:10.1029/97GL00861
460 Hornig-Kjarsgaard I, Keller J, Koberski U, Stadlbauer E, Francalanci L, Lenhart R (1993) Geology,
461 stratigraphy and volcanological evolution of the island of Stromboli, Aeolian arc, Italy. Acta
462 Vulcanologica 3:21-68
463 Istitituto Nazionale di Geofisica e Vulcanologia (INGV) – Centro Nazionale Terremoti. Online earthquake
464 database available at: http://cnt.rm.ingv.it.
465 Keller J, Hornig-Kjarsgaard I, Koberski U, Stadlbauer E, Francalanci L, Lenhart R (1993) Geological Map
466 of the Island of Stromboli. Acta Vulcanologica
467 Landi P, Corsaro RA, Francalanci L, Civetta L, Miraglia L, Pompilio M, Tesoro R (2009) Magma dynamics
468 during the 2007 Stromboli eruption (Aeolian Islands, Italy): Mineralogical, geochemical and isotopic
469 data. J Volcanol Geotherm Res 182(3-4):255-268. doi:10.1016/j.jvolgeores.2008.11.010
470 Landi P, Métrich MN, Bertagnini A, Rosi M (2004) Dynamics of magma mixing and degassing recorded
471 in plagioclase at Stromboli (Aeolian Archipelago, Italy). Contrib Mineral Petrol 147:213–227.
472 doi:10.1007/s00410-004-0555-5
473 Marchetti E, Genco R, Ripepe M (2009) Ground deformation and seismicity related to the propagation and
474 drainage of the dyke feeding system during the 2007 effusive eruption at Stromboli volcano (Italy).
475 J Volcanol Geotherm Res 182(3-4):155-161. doi:10.1016/j.jvolgeores.2008.11.016
476 Marchetti E, Ripepe M (2005) Stability of the seismic source during effusive and explosive activity at
477 Stromboli Volcano. Geophys Res Lett 32: L03307. doi:10.1029/2004GL021406
478 Marsella M, Baldi P, Coltelli M, Fabris M (2011) The morphological evolution of the Sciara del Fuoco
479 since 1868: reconstructing the effusive activity at Stromboli volcano. Bull Volcanol 74:231–248.
480 doi:10.1007/s00445-011-0516-6

Métrich N, Bertagnini A, Landi P, Rosi M (2001) Crystallization driven by decompression and water loss at Stromboli volcano (Aeolian Islands, Italy). J Petrol 42(8):1471-1490. doi:10.1093/petrology/42.8.1471

Métrich N, Bertagnini A, Di Muro A (2009) Conditions of magma storage, degassing and ascent at Stromboli: New insights into the volcano plumbing system with inferences on the eruptive dynamics. J Petrol 51(3):603-626. doi:10.1093/petrology/egp083

Patrick MR, Anderson KR, Poland MP, Orr T, Swanson DA (2015) Lava lake level as a gauge of magma reservoir pressure and eruptive hazard. Geology 43:831–834. doi: 10.1130/G36896.1

Pioli L, Pistolesi M, Rosi M (2014) Transient explosions at open-vent volcanoes: The case of Stromboli (Italy). Geology 42(10):863-866. doi:10.1130/G35844.1

Pistolesi M, Delle Donne D, Pioli L, Rosi M, Ripepe M (2011) The 15 March 2007 explosive crisis at Stromboli volcano, Italy: assessing physical parameters through a multidisciplinary approach. J Geophys Res 116, B12206. doi:10.1029/2011JB008527

Ripepe M, Delle Donne D, Genco R, Maggio G, Pistolesi M, Marchetti E, Lacanna G, Ulivieri G, Poggi P (2015) Volcano seismicity and ground deformation unveil the gravity-driven magma discharge dynamics of a volcanic eruption. Nat. Commun 6:6998. doi:10.1038/ncomms7998

Ripepe M, Delle Donne D, Lacanna G, Marchetti E, Ulivieri G (2009) The onset of the 2007 Stromboli effusive eruption recorded by an integrated geophysical network. J Volcanol Geotherm Res 182(3-4):131-136. doi:10.1016/j.jvolgeores.2009.02.011

Ripepe M, Marchetti E, Poggi P, Harris AJL, Fiaschi A, Ulivieri G (2004) Seismic, Acoustic, and Thermal Network Monitors the 2003 Eruption of Stromboli Volcano. Eos 85(35):329–336

Ripepe M, Marchetti E, Ulivieri G (2007) Infrasonic monitoring at Stromboli volcano during the 2003 effusive eruption: Insights on the explosive and degassing process of an open conduit system. J Geophys Res 112:B09207. doi:10.1029/2006JB004613

Ripepe M, Marchetti E, Ulivieri G, Harris A, Dehn J, Burton M, Caltabiano T, Salerno G (2005) Effusive to explosive transition during the 2003 eruption of Stromboli volcano. Geology 33(5):341-344. doi:10.1130/G21173.1

Rosi M (1980) The island of Stromboli. Rend. Soc. It. Min. Pet. 36:345–368

Rosi M, Bertagnini A, Landi P (2000) Onset of the persistent activity at Stromboli Volcano (Italy). Bull Volcanol 62(4-5):294-300. doi:10.1007/s004450000098

Rosi M, Bertagnini A, Harris AJL, Pioli L, Pistolesi M, Ripepe M (2006) A case history of paroxysmal explosion at Stromboli: timing and dynamics of the April 5, 2003 event. Earth Planet Sci Lett 243:594–606

Rosi M, Pistolesi M, Bertagnini A, Landi P, Pompilio M, Di Roberto A (2013) Stromboli volcano, Aeolian Islands (Italy): present eruptive activity and hazards. In: Lucchi F, Peccerillo A, Keller J, Tranne CA, Rossi PL (ed), The Aeolian Islands Volcanoes, Geological Society, London, Memoirs, 37:473–490. doi:10.1144/M37.14

Stevenson DS, Blake S (1998) Modelling the dynamics and thermodynamics of volcanic degassing. Bull Volcanol 60:307–317. doi:10.1007/s004450050234

Tibaldi A (2001) Multiple sector collapses at Stromboli volcano, Italy: how they work. Bull Volcanol 63:112–125. doi:10.1007/s004450100129

Tinti S, Maramai A, Armigliato A, Graziani L, Manucci A, Pagnoni G, Zaniboni F (2006) Observations of physical effects from tsunamis of December 30, 2002 at Stromboli volcano, southern Italy. Bull Volcanol 68:450-461. doi:10.1007/s00445-005-0021-x

Zakšek K, Hort M, Lorenz E (2015) Satellite and Ground Based Thermal Observation of the 2014 Effusive Eruption at Stromboli Volcano. Remote Sens 7:17190-17211. doi:10.3390/rs71215876

Figure 1

Click here to download Figure fig_01.png

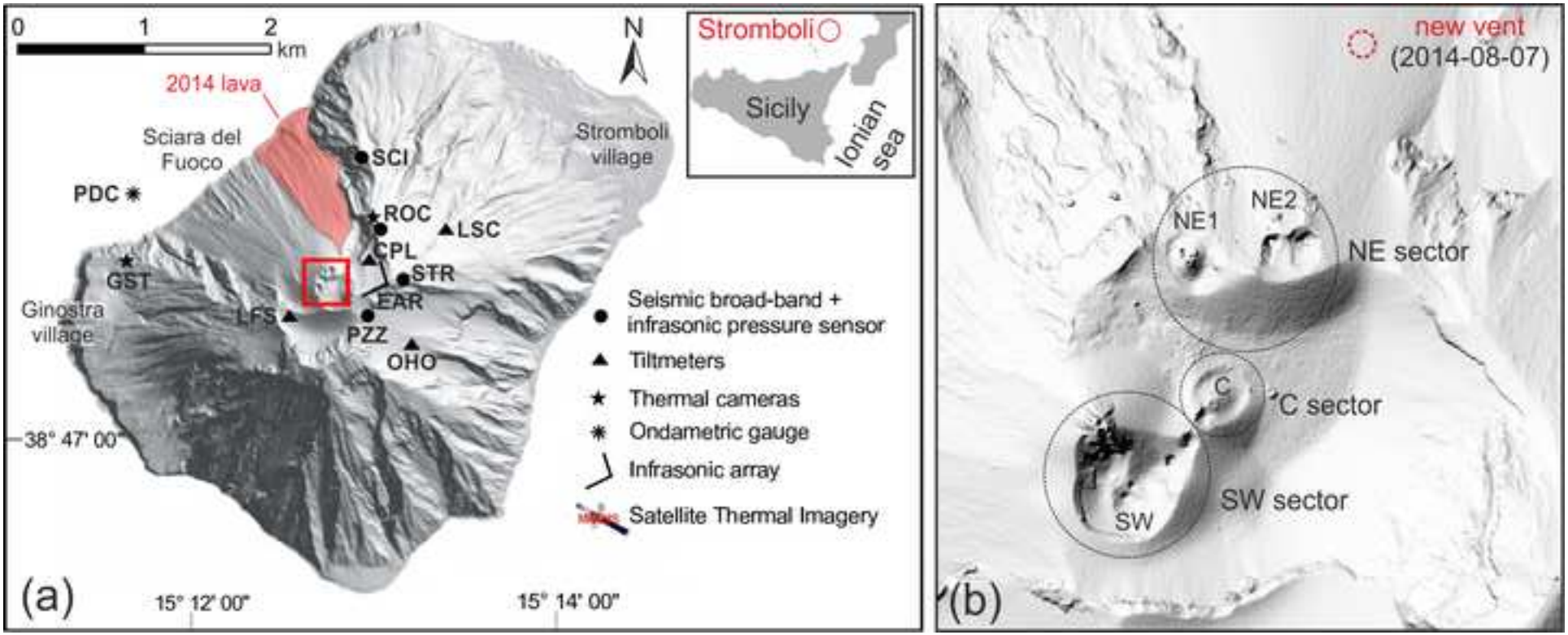

Figure 2

Click here to download Figure fig_02.png

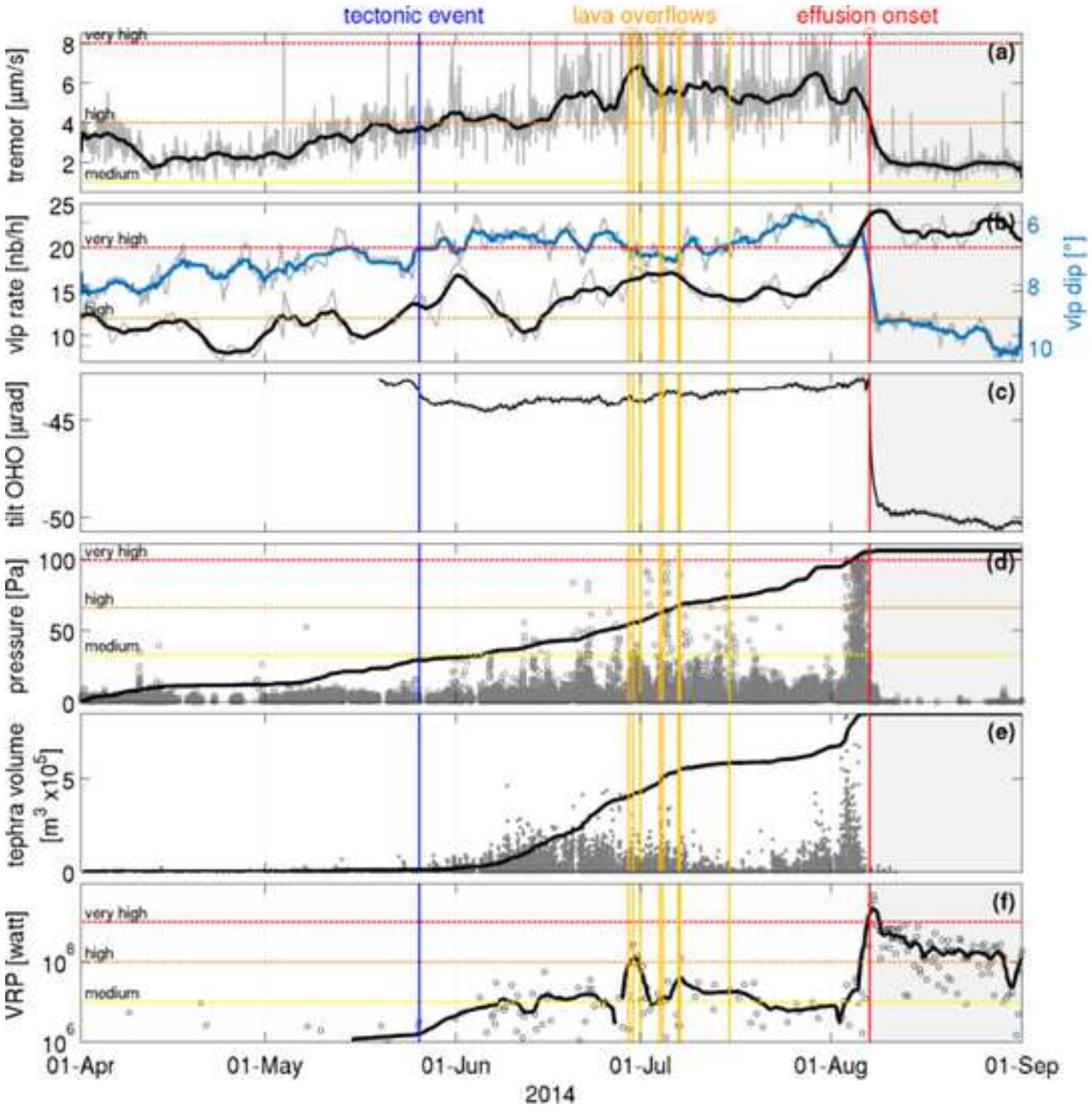

Figure 3

Click here to download Figure fig_03.png

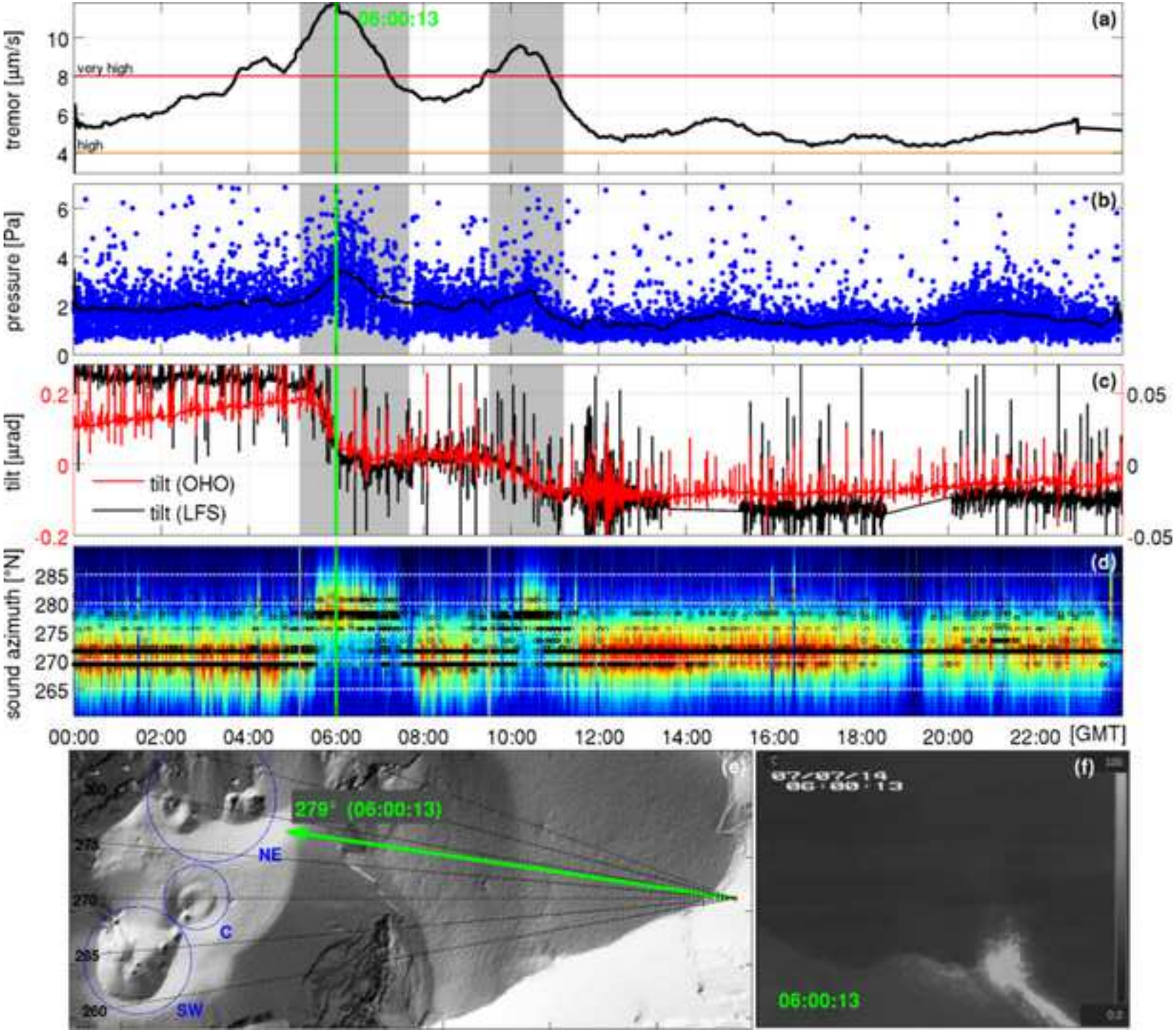

Figure 4

Click here to download Figure fig_04.png

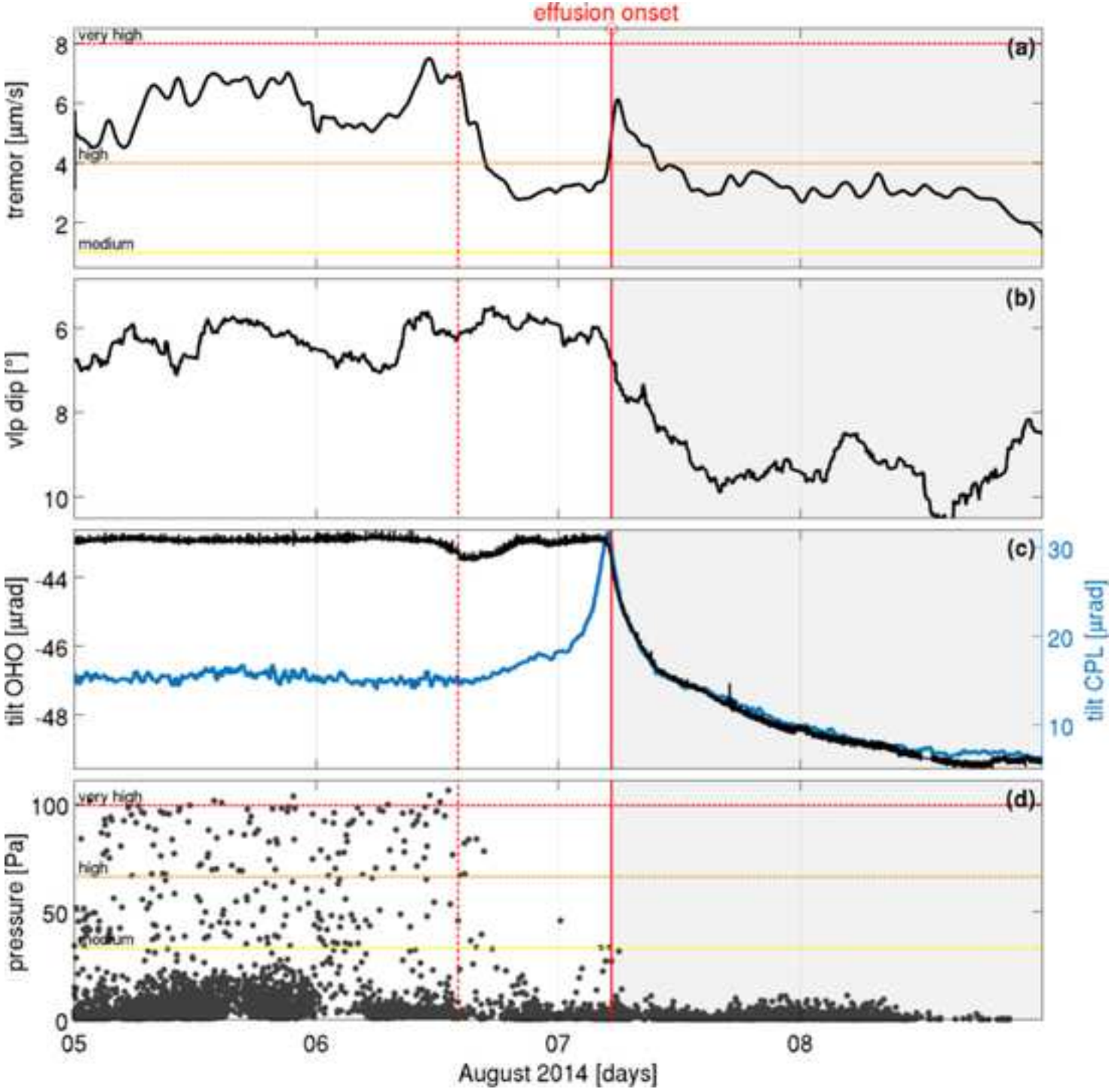

Figure 5

Click here to download Figure fig_05.png

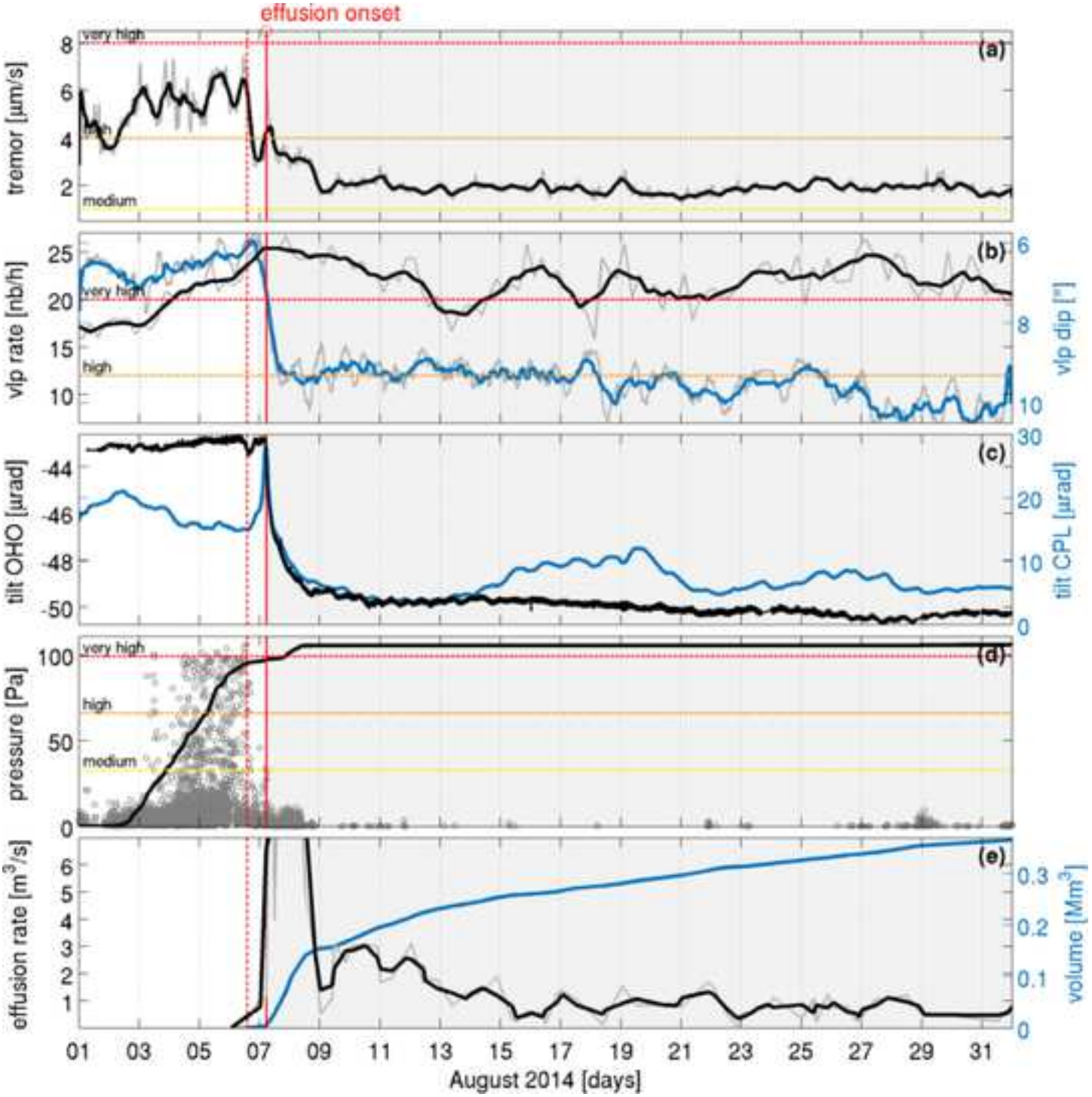

Figure 6

Click here to download Figure fig_06.png

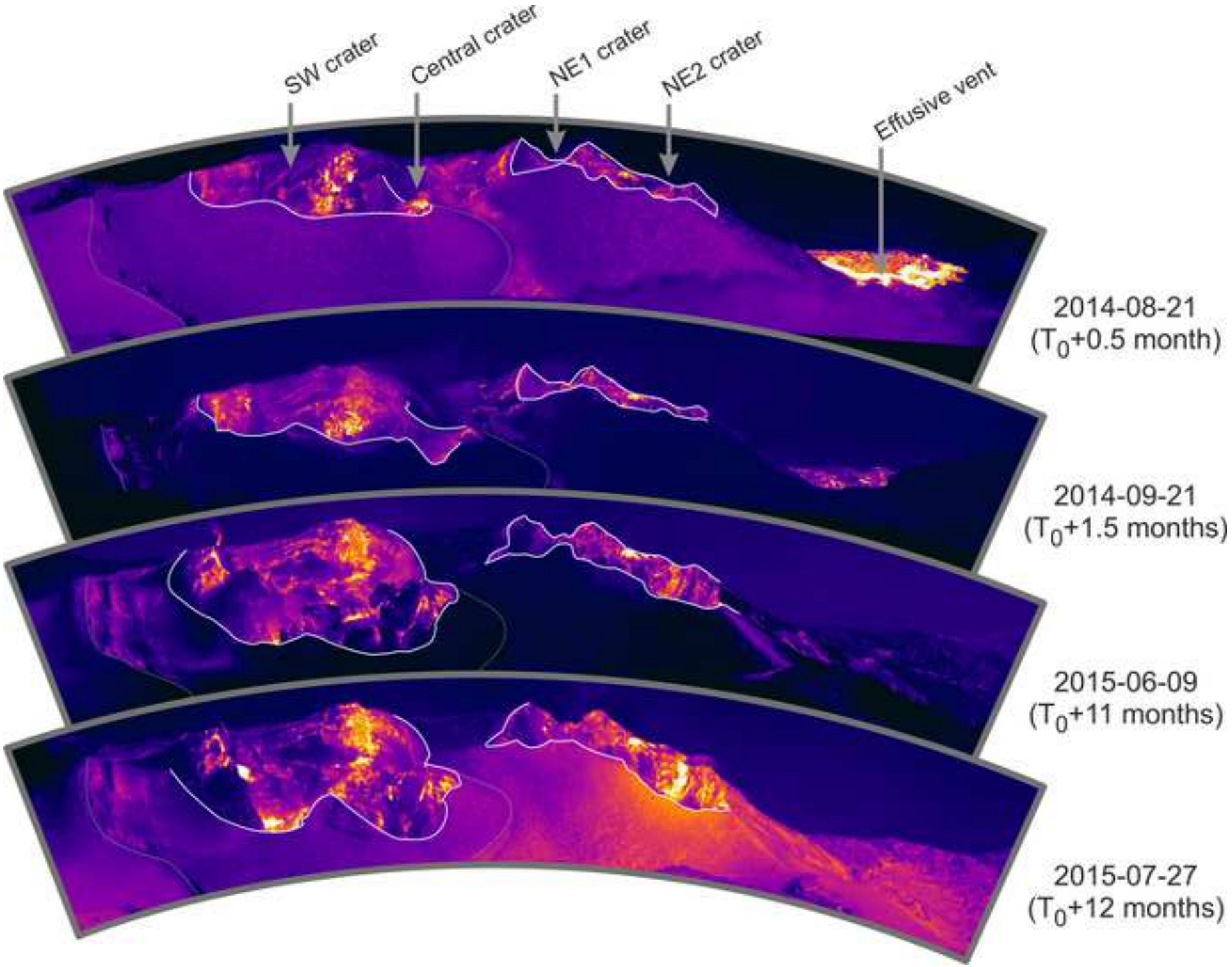

Figure 7

Click here to download Figure fig_07.png

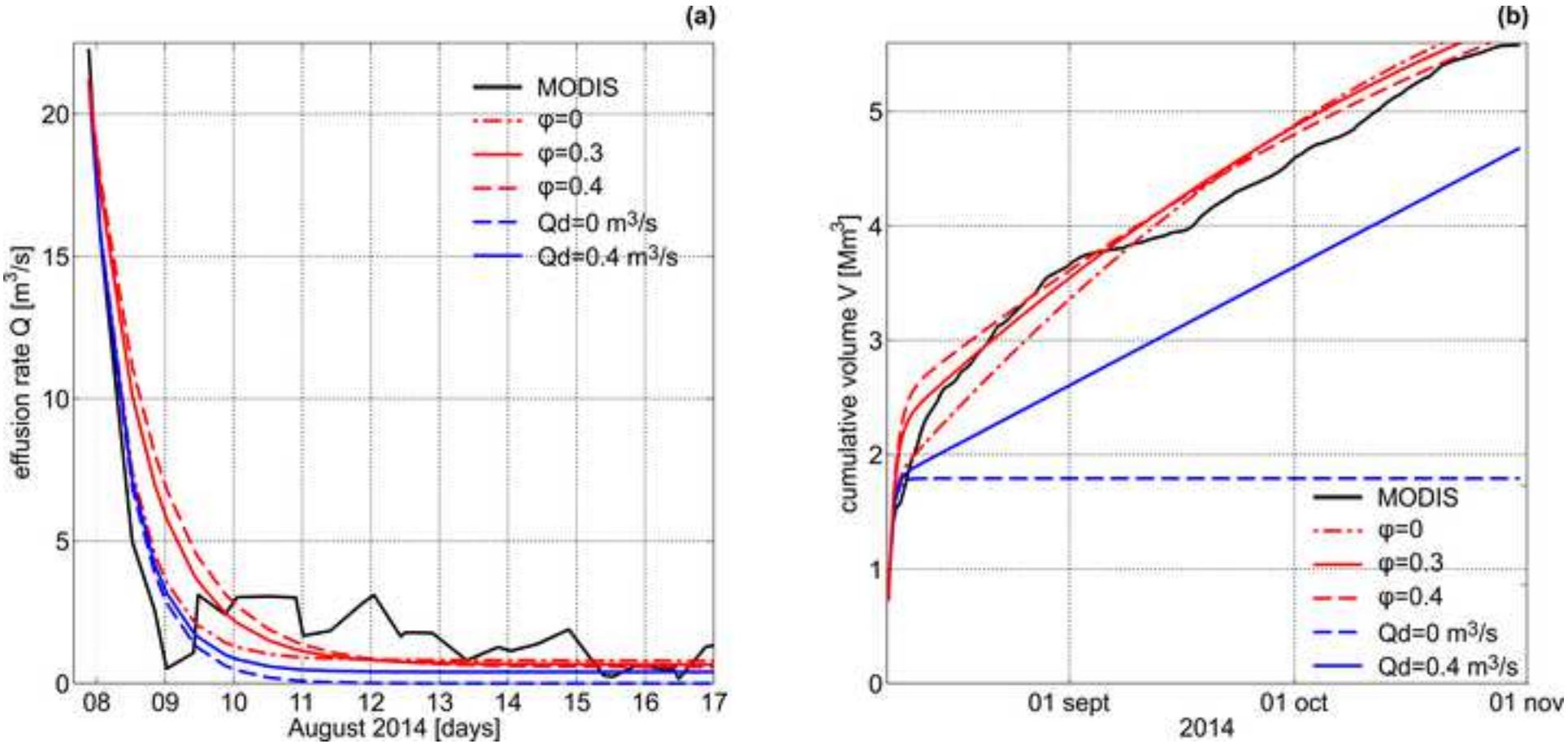

Figure 8

Click here to download Figure fig_08.png

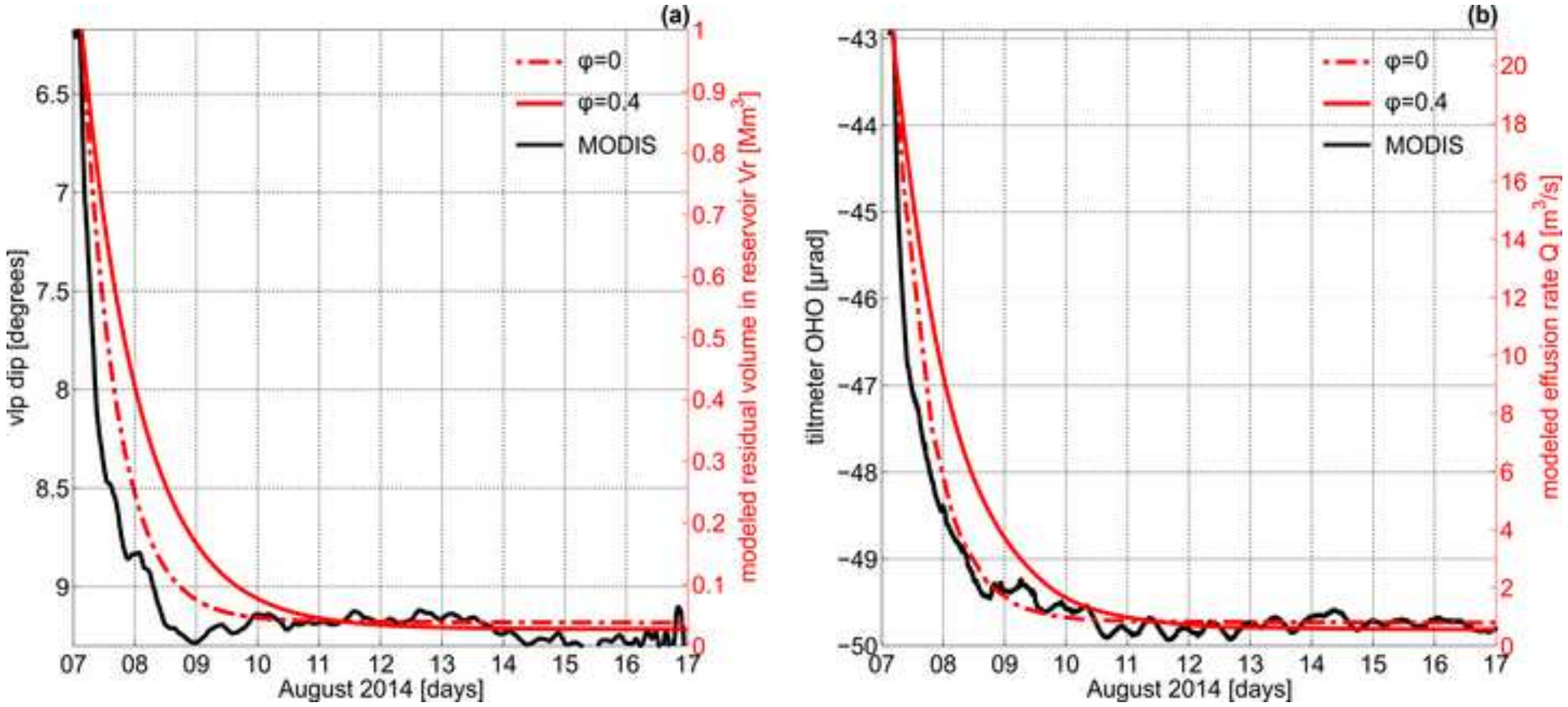

Figure 9

Click here to download Figure fig_09.png